

## Far-Infrared Spectra of Erbium, Dysprosium, and Samarium Ethyl Sulphate\*†

J. C. HILL‡ AND R. G. WHEELER

*Sloane Physics Laboratory, Yale University, New Haven, Connecticut*

(Received 20 June 1966)

A far-infrared interferometric spectrometer has been used to make the first direct observation of transitions between the Stark- and Zeeman-split ground  $J$  manifolds of rare-earth ions in ethyl sulphate crystals. The description of both the Stark and Zeeman splittings in terms of crystal-field theory has been considered, and the data obtained here have proved sufficient for making an accurate evaluation of the parameters contained in the theory. The intensities of the observed transitions have been investigated and it has been found that they are primarily magnetic-dipole transitions. However, significant deviations between calculation and observation occurred for both the splittings and line intensities. A hypothesis has been developed by which both kinds of discrepancies are attributed to interaction between the rare-earth-ion electronic states and the phonons or lattice waves in the ethyl sulphate crystals.

### INTRODUCTION

WHEN a rare-earth ion is placed in a crystal its energy levels or  $J$  manifolds undergo a Stark splitting in the electric field produced by the surrounding ions in the lattice. The components of a split manifold are separated on the order of  $100\text{ cm}^{-1}$ , giving rise to energy differences which lie in the far-infrared region of the spectrum. The Stark splitting of the ground  $J$  manifold is of particular interest, because to this date only indirect measurements of this splitting have been made. With the use of a far-infrared interferometric spectrometer it has been possible to make the first observations of transitions between the Stark components of ground  $J$  manifolds of rare-earth ions in ethyl sulphate crystals. By applying magnetic fields up to 80 kG to the crystals, the Zeeman splitting of the Stark levels has also been observed. Both the Stark and Zeeman splitting are describable by crystal-field theory, and the data obtained here has been used to make an accurate evaluation of the crystal-field parameters contained in this theory.

### EXPERIMENTAL TECHNIQUES

The far-infrared spectra were obtained with a system built around a commercially available interferometric spectrometer.<sup>1</sup> The design of the system and the general experimental techniques have been described elsewhere.<sup>2</sup>

In order to ensure the temperature of the sample crystals being well known, they are immersed directly in liquid helium. In different runs the sample temperature ranged from 1.57 to 1.65°K, a variation which produced no observable changes in any of the spectra.

A superconducting solenoid was used to apply mag-

netic fields up to 80 kG to the samples. The field is measured to an accuracy of  $\pm 1\%$  using a magneto-resistance probe constructed of commercial copper wire.

The crystals are grown by evaporation of the rare-earth ethyl sulphate hydrous solution at about 35°C from which clear single crystals of the concentrated salt are obtained. Samples of crystals used to obtain data were subjected to spectroscopic analysis and were found to be 99.99% pure, with admixtures of other rare earths being in the 0.01% range or less. The crystals run were thin disks 0.1 to 0.2 mm thick and were cut from the crystals as grown with a jeweler's saw, then thinned down by water etching on wet filter paper. In the magnetic field work it was necessary to have the crystal  $c$  axis accurately aligned with respect to the field. For the  $\mathbf{H}\parallel c$  case where the  $c$  axis was normal to the plane of the disk, a polarizing microscope and Bertrand lens were used to measure any misalignment of crystals when they were supported in their holder. When any misorientation of the holder in the light pipe and of the light pipe with respect to the magnet are taken into account, the misalignment is typically less than 2°. For  $\mathbf{H}\perp c$  crystals, where the  $c$  axis is parallel to the plane of the disk, the Bertrand lens could not be used, but disks were cut parallel to flats which developed on the growing crystals. Since the flats grow parallel to the hexagonal  $c$  axis, the orientation is estimated to be at least as good as for the  $\mathbf{H}\parallel c$  case.

### PHONONS

The ethylsulphates studied not only contained absorption lines corresponding to transitions between Stark levels of the rare-earth ions, but also lines produced by the excitation of lattice waves or phonons. Geserich *et al.*<sup>3</sup> have investigated the near and medium infrared reflection and Raman spectra of lanthanum ethyl sulphate between 300 and 4000  $\text{cm}^{-1}$  and have correlated all but two Raman lines at 296 and 357  $\text{cm}^{-1}$  with internal motions of the water molecules of hydra-

\* Work supported in part by The National Science Foundation.

† Based on a thesis presented to the faculty of the Graduate School of Yale University in partial fulfillment of the requirements for the Ph.D. degree by J. C. Hill.

‡ Present address: General Motors Research Laboratories, Warren, Michigan.

<sup>1</sup> Sir Howard Grubb Parsons and Company, Ltd., Walkergate, Newcastle upon Tyne 6, England.

<sup>2</sup> R. G. Wheeler and J. C. Hill, *J. Opt. Soc. Am.* **56**, 657 (1966).

<sup>3</sup> H. P. Geserich, K. H. Hellwege, and G. Schaack, *Z. Naturforsch.* **20a**, 289 (1965).

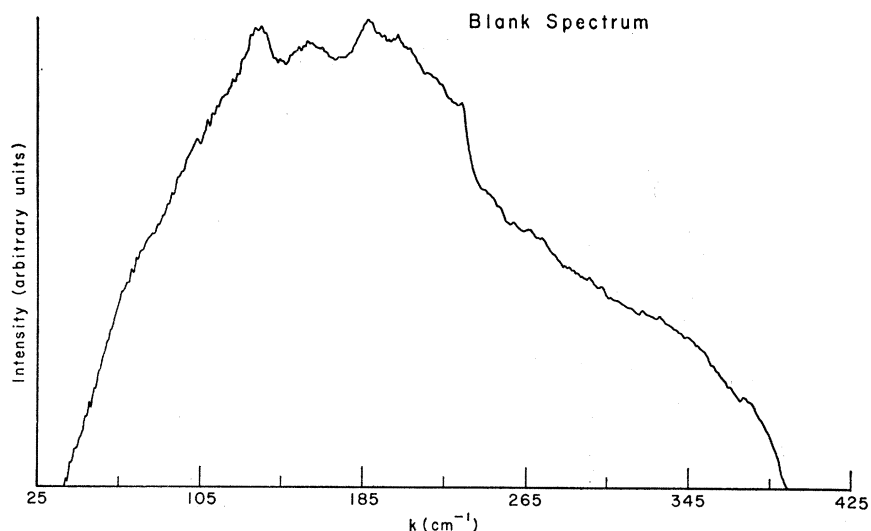


FIG. 1. Blank spectrum, i.e., no sample in the beam, showing the spectral distribution of energy at the detector.

tion and the ethyl and sulphate complexes. Since the distances between the rare-earth ions, water molecules and ethyl and sulphate radicals, each moving as a unit, are much larger than the distances within the molecules and radicals themselves, one expects several more modes to appear at lower frequencies. This is indeed the case as shown by Wong and Erath,<sup>4</sup> who have observed a total of 42 phonon modes at frequencies under  $400\text{ cm}^{-1}$  coupled to electronic transitions in the visible and near infrared in the ethyl sulphates of neodymium, erbium, and praseodymium.

In order to aid the separation of observed absorption lines into phonon and crystal field lines, a spectrum was obtained for lanthanum ethyl sulphate, in which the

diamagnetic lanthanum has no  $4f$  electrons and therefore no Stark levels. To provide a point of reference a spectrum with no sample in the beam is shown in Fig. 1, and in the following Fig. 2 is shown a lanthanum spectrum where the phonon lines have been labeled  $P_1$ - $P_{14}$ . The highest lying mode at  $\approx 360\text{ cm}^{-1}$  is not well located because it is broad and the transmission of the beamsplitter is rapidly dropping to zero at this point, with the result that only the lower portion of the line can be seen. However, comparison with the blank spectrum definitely confirms the presence of an absorption line in this region. When working with thicker beamsplitters which transmit more energy at low frequencies, an indication has been found that there is

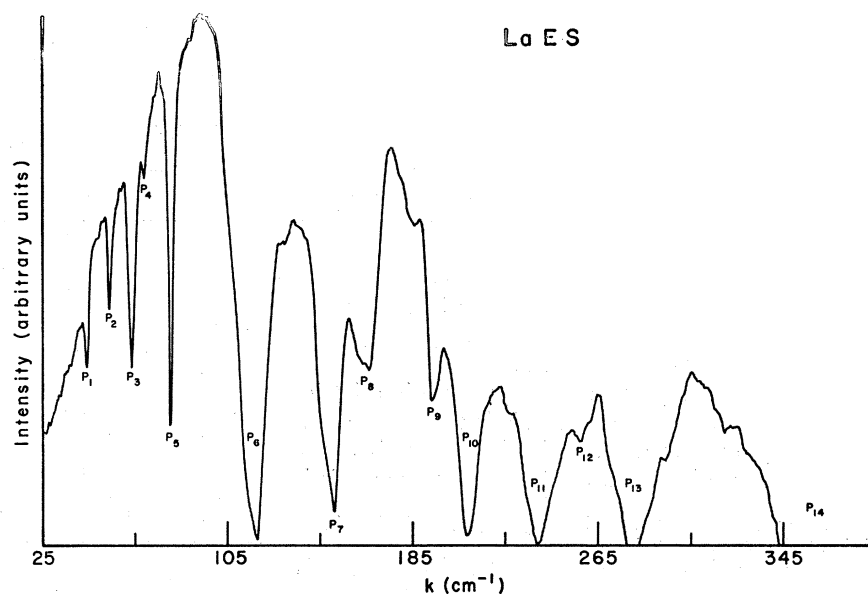


FIG. 2. Lanthanum-ethyl sulphate (LaEs) spectrum with absorption lines  $P_1$ - $P_{14}$  produced by the excitation of phonons.

<sup>4</sup> Eugene Y. Wong and Edward H. Erath, J. Chem. Phys. 39,1629 (1963).

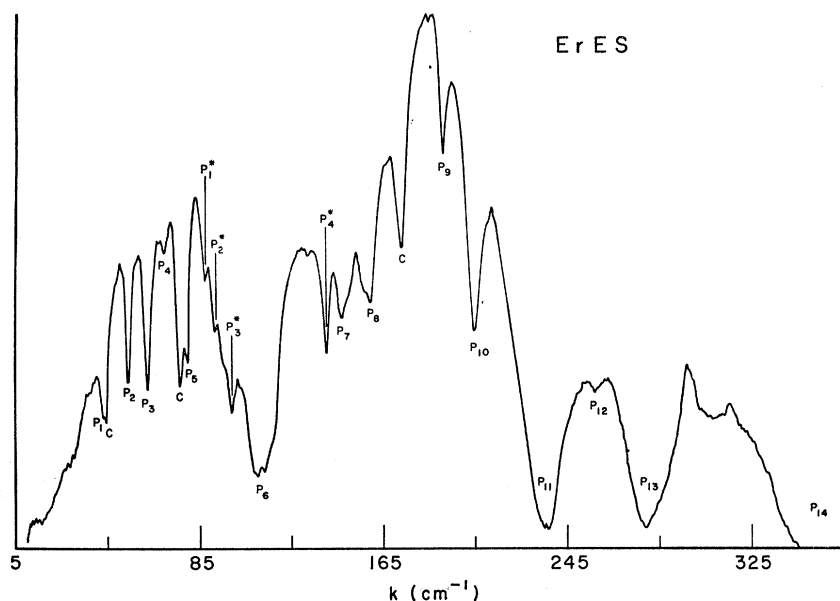


FIG. 3. Erbium-ethyl sulphate (ErES) spectrum with phonon lines labeled  $P_1$ - $P_{14}$ . The lines labeled with a  $C$  are crystal field lines while those labeled  $P_1^*$ - $P_4^*$  are the additional phonon lines.

still another mode at about  $6 \text{ cm}^{-1}$ , but the existence of this mode is still uncertain. To check if this number of modes is reasonable, a factor group analysis of the type described by several authors<sup>5-7</sup> has been made.

This analysis is essentially a process of determining how many phonons or normal modes of a given type are allowed by the symmetry and number of particles in a system. It begins by recognizing the fact that the normal modes must transform as the symmetry group  $G$  of the crystal in which they exist, i.e., they form a set of basis vectors for a representation of  $G$ , and this representation is called the representation of the motions. Now here the modes of interest are the infrared active modes, since they are the ones which produce the observed absorption. The excitation of an initial state  $\psi_i$  to the state  $\psi_f$  will be an electric dipole transition, i.e., infrared active, if the representation of  $\psi_i^* \psi_f$  contains a representation  $\Gamma_V$  of a vector. One then determines how these infrared active modes transform under  $G$ , i.e., determines for which irreducible representations of  $G$  they form a basis. The number of times these particular irreducible representations are contained in the representation of the motions is then equal to the number of this particular kind of mode, i.e., infrared active mode, in the total number of modes which can be active in the system.

The rare-earth ethyl sulphates crystallize in a lattice which has symmetry  $C_{6h}^2$ , and this is  $G$  for our case.<sup>8</sup> The underlying point group which is isomorphic to the factor group considered in the factor group analysis is

<sup>5</sup> S. Bhagavantam and F. Venkatarayudu, Proc. Indian Acad. Sci. **9A**, 224 (1939).

<sup>6</sup> Harvey Winston and Ralph S. Halford, J. Chem. Phys. **17**, 607 (1949).

<sup>7</sup> S. A. Pollack, J. Chem. Phys. **38**, 98 (1963).

<sup>8</sup> J. A. A. Ketelaar, Physica **4**, 619 (1937).

$C_{6h}$ . Character tables for  $C_{6h}$  are found in Koster *et al.*,<sup>9</sup> where the designation + and - for even and odd representations will here be changed to  $g$  (gerade) and  $u$  (ungerade), respectively. Since the normal modes are expressible in Cartesian coordinates only and do not contain spinors, the operation  $\bar{E}$  is the same as  $E$  and only the portion of the table corresponding to an even number of electrons need be considered. It can easily be shown that only  $\Gamma_{1u}$ ,  $\Gamma_{5u}$ , and  $\Gamma_{6u}$  transform as a vector, however,  $\Gamma_{5u}$  and  $\Gamma_{6u}$  are related by time reversal and Koster *et al.*<sup>9</sup> show that the functions transforming according to these two representations must degenerate in pairs.

In accordance with Geserich *et al.*<sup>3</sup> it is now assumed that the rare-earth ions, water molecules, ethyl radicals,

TABLE I. Phonon absorption frequencies (in  $\text{cm}^{-1}$ ) for lanthanum, erbium, dysprosium, and samarium ethyl sulphate.

Phonon	La	Er	Dy	Sm
$P_1$	44.7	44.2	44.1	44
$P_2$	54	54.6	54.1	51.7
$P_3$	63.6	63	62.7	61.5
$P_4$	69.2	70	70	70.6
$P_5$	80.5	80	79.2	77.9
$P_6$	117.5	110.5	112	
$P_7$	150	148	143.5	
$P_8$	165.5	159	155.5	
$P_9$	194.5	192	190.5	
$P_{10}$	209	205	207	
$P_{11}$	240	237	241	
$P_{12}$	259	258.5	258	
$P_{13}$	282	284	286.5	
$P_{14}$	$\approx 360$	$\approx 360$	$\approx 360$	

<sup>9</sup> G. F. Koster, J. O. Dimmock, R. G. Wheeler, and H. Statz, *Properties of the Thirty-Two Point Groups* (MIT Press, Cambridge, Massachusetts, 1963).

and sulphate radicals all move as units. There are then 16 particles in a molecule and since there are two molecules per unit cell, a total of 32 particles per unit cell. By a straightforward application of the factor group analysis in which account is taken of translation modes of the crystal as a whole, it is found that there are six  $\Gamma_{1u}$  and nine  $\Gamma_{5u}(\Gamma_{6u})$  infrared active modes. The total of fifteen is consistent with the observation of fourteen, and possibly fifteen, modes.

Modes similar to those in the lanthanum salt were also observed in erbium and dysprosium ethyl sulphate, and in the investigated region below  $100\text{ cm}^{-1}$  in samarium ethyl sulphate. An example is shown in the erbium spectrum in Fig. 3, where the modes corresponding to those in Fig. 2 for the lanthanum are again labeled  $P_1$ - $P_{14}$ . The additional lines labeled with a  $C$  are crystal-field lines and will be considered later. The frequencies of these modes for all four ethyl sulphates are listed in Table I, where it can be seen that they vary little from salt to salt. This is to be expected, since the nature of the particles and the distances between them are very similar in all the crystals. However, referring again to Fig. 3, there are four additional absorption lines labeled  $P_1^*$ - $P_4^*$ , which were not observed in lanthanum ethyl sulphate. The origin of these lines is not clear, but they also appear to be phonons, possibly localized impurity modes of the type described by Maradudin *et al.*<sup>10</sup> These lines do not shift at all when a magnetic field up to 80 kG is applied, while all the crystal-field lines do shift. In addition, the three lines  $P_1^*$ ,  $P_2^*$ , and  $P_3^*$  were observed in all three magnetic salts, including samarium where all Stark levels were also observed. Although the  $141\text{-cm}^{-1}$  line was observed only in erbium, it was not possible to obtain a fit to the levels using crystal-field theory when this line was assumed to belong to a Stark level. It thus appears clear that all four of these lines are additional phonon modes, but since the factor group analysis given above indicates at most one of these can be a lattice mode, they are probably impurity modes. For completeness they are listed in Table II.

### THEORY

We write the Hamiltonian  $H$  for a rare-earth ion in an ethyl sulphate lattice as

$$H = H_{es} + H_{sl} + V_c + H_z,$$

where  $H_{es}$  represents the electrostatic interactions within an ion,  $H_{sl}$  the spin-orbit interaction,  $V_c$  the energy of the ion in the crystalline electric field, and  $H_z$  the Zeeman term for an applied magnetic field.<sup>11</sup> The first two terms  $H_{es} + H_{sl}$  give rise to a set of energy

TABLE II. Absorption frequencies (in  $\text{cm}^{-1}$ ) for the additional phonon modes in erbium, dysprosium, and samarium ethyl sulphate.

Phonon	Er	Dy	Sm
$P_1^*$	87.8	87.4	86.2
$P_2^*$	92.4	92	91.4
$P_3^*$	99.4	99.2	98.3
$P_4^*$	141		

levels or  $J$  manifolds for which  $J$  and  $J_z$  are good quantum numbers, but which are degenerate in the  $2J+1$  values of  $J_z$ . The spin-orbit interaction prevents  $L$  and  $S$  being good quantum numbers, but the ground  $J$  manifolds of rare-earth ions are typically 95% pure Russell-Saunders states. We therefore make the approximation that  $L$  and  $S$  are good quantum numbers and designate the states by  $\psi(L, S, J, J_z)$ . The addition of  $V_c$  causes the  $J$  manifolds to split into Stark levels, which to first order are linear combinations over  $J_z$  of the  $\psi(L, S, J, J_z)$ . These combinations in turn determine how the Stark levels split when a magnetic field is applied, so that both the Stark and Zeeman splitting depend on  $V_c$ .

Elliott and Stevens<sup>12-14</sup> have developed a crystal-field theory and applied it specifically to the case of a rare-earth ion in an ethyl sulphate lattice.  $V_c$  is written as

$$V_c = \sum_{l,m} A_l^m \sum_i r_i^l Y_l^m(\theta_i, \varphi_i), \quad (1)$$

where  $r_i$ ,  $\theta_i$ , and  $\varphi_i$  are the coordinates of the  $i$ th  $4f$  electron and the  $A_l^m$  are parameters to be determined empirically as characterizing the crystalline field. By considering the character of the wave functions between which matrix elements of  $V_c$  are calculated and the  $C_{3h}$  site symmetry of the rare-earth ion<sup>8</sup> the number of terms can be reduced to those containing the parameters  $A_2^0$ ,  $A_4^0$ ,  $A_6^0$ , and  $A_6^6$ .

Matrix elements of  $V_c$  can be calculated using the operator equivalent technique of Stevens<sup>15</sup> and Elliott and Stevens.<sup>13,14</sup> Each of the sums of one electron terms in  $V_c$  is shown to have matrix elements that are proportional to the product of an operator equivalent  $O(J)$  and an operator equivalent factor  $F(L, S, J, l)$ , i.e.,

$$\begin{aligned} \langle L, S, J, J_z | \sum_i r_i^l Y_l^m(\theta_i, \varphi_i) | L, S, J, J_z \rangle \\ = \langle r_l \rangle_{4f} F(L, S, J, l) O(J), \quad (2) \end{aligned}$$

where the  $\langle r^l \rangle_{4f}$  are averages of the  $r^l$  over the  $4f$  radial wave functions. Since these functions are not well known, the  $\langle r^l \rangle_{4f}$  are absorbed into the  $A_l^m$  to define

<sup>12</sup> R. J. Elliott and K. W. H. Stevens, Proc. Roy. Soc. (London) **A215**, 437 (1952).

<sup>13</sup> R. J. Elliott and K. W. H. Stevens, Proc. Roy. Soc. (London) **A218**, 553 (1953).

<sup>14</sup> R. J. Elliott and K. W. H. Stevens, Proc. Roy. Soc. (London) **A219**, 387 (1953).

<sup>15</sup> K. W. H. Stevens, Proc. Phys. Soc. (London) **A65**, 209 (1952).

<sup>10</sup> A. A. Maradudin, E. W. Montroll, and G. H. Weiss, *Theory of Lattice Dynamics in the Harmonic Approximation* (Academic Press Inc., New York, 1963).

<sup>11</sup> B. G. Wybourne, *Spectroscopic Properties of Rare Earths* (John Wiley and Sons, Inc., New York, 1965).

new parameters  $B_i^m$  by

$$B_i^m = A_i^m \langle r^l \rangle_{4f}. \quad (3)$$

Using this technique all first-order matrix elements of  $V_e$  can be calculated easily.

However,  $V_e$  also has matrix elements between manifolds of different  $J$ . Elliott and Stevens<sup>14</sup> interpret the results of resonance experiments on dilute samarium ethyl sulphate in terms of a small admixture of the excited  $J = \frac{7}{2}$  manifold at  $\approx 1000 \text{ cm}^{-1}$  into the ground  $J = \frac{5}{2}$  manifold. Even though the admixture is small, it must be included to obtain a good fit to the data. It is then to be expected that the same procedure will have to be followed here. For the sake of consistency it was decided to perform such a second-order calculation for all three ions, but since the effects are not large, only interaction with the nearest excited manifold is considered. Matrix elements of  $V_e$  among the excited states and between the manifolds can also be calculated by the operator equivalent technique. Operator-equivalent factors for the latter elements are given by Elliott and Stevens.<sup>13</sup> Operator equivalent factors for elements within the excited manifolds were obtained from tables in Prather.<sup>16</sup> He uses the tensor operator technique in which matrix elements are written as products of Wigner coefficients and reduced matrix elements. However, the reduced matrix elements are directly related to the operator equivalent factors used here, and the former can be converted to the latter by taking account of normalization constants.

For the case where a magnetic field  $\mathbf{H}$  is applied the matrix elements of the additional term  $H_z$  in the Hamiltonian are added to the matrix. We have

$$H_z = g_L \beta \mathbf{H} \cdot \mathbf{J}, \quad (4)$$

where  $g_L$  is the Lande  $g$  factor and  $\beta$  the Bohr magneton. Matrix elements of  $H_z$  within a  $J$  manifold are easily calculated and tables in Elliott and Stevens<sup>13</sup> give the operator equivalents and  $g_L$  for elements between manifolds.

At this point the treatment of intermediate coupling should be considered. The admixing of states with the same  $J$  but different  $L$  and  $S$  will not affect the operator equivalents, but will change the operator equivalent factors. The operator equivalent factors combine with the  $B_i^m$  in such a way that to first order a change in the factors can be accommodated by scaling the  $B_i^m$  to the same extent as the factors change. The scaling will generally be different for an excited manifold, but again this will be a small effect. It will later be seen that the second-order calculation produces small changes over a first-order calculation, so to second-order treating the parameters as being scaleable will amount to neglecting a small correction of a small correction.

Once the entire second-order matrix for a given ion is calculated with the  $B_i^m$  as parameters, the best available values of the  $B_i^m$  are inserted and the matrix diagonalized on an IBM 7094/7040 computer. The calculated energy levels are used to obtain transition energies corresponding to the transitions observed and the calculated and observed results are compared. The computer is then used to perform a least-squares analysis, in which a set of changes in the parameters is found which minimizes the sum  $\Sigma$  of the squares of the differences between calculated and observed transition energies. The parameter changes are used to obtain new parameters, and the whole process is repeated. In practice it has been found that a few iterations are sufficient to obtain the minimum value of  $\Sigma$ , and the parameters so obtained are taken to be the best-fit parameters.

For several years the intensities of spectral lines in rare-earth compounds have been of interest, primarily because they could not be explained as simple first-order electric dipole transitions. States  $\psi_i$  and  $\psi_j$  arising from a pure  $4f^n$  configuration must have the same parity, while  $\mathbf{r}$  has odd parity, so that the electric dipole transition matrix element  $\int \psi_i^* \mathbf{r} \psi_j d\tau$  must be zero. Several authors<sup>17-22</sup> have discussed mechanisms by which the observation of many spectral lines in rare-earth compounds may be explained. The explanations fall into four categories: (1) admixtures by odd terms in the crystalline field of states from excited configurations with parity opposite to the ground configuration, (2) coupling of vibronic states of the crystal or phonons with the electronic states, (3) presence of magnetic dipole transitions, and (4) presence of electric quadrupole transitions. It will be shown that observed transitions within the ground manifolds of the ions studied can be correlated best with (3) above, but with some additional type-(2) contributions.

Broer *et al.*<sup>18</sup> estimate transition probabilities for both electric quadrupole and magnetic dipole transitions between different  $J$  manifolds and find the probabilities are nearly equal. For transitions within a manifold, which is the case of interest here, the magnetic dipole transition probability will be much greater. Estimates of electric quadrupole matrix elements show they are approximately the same for inter- and intramanifold transitions, while magnetic dipole matrix elements are larger for transitions within a  $J$  manifold, since they do not require admixing of different  $J$  manifolds to be non-zero. Furthermore, the electric quadrupole transition probabilities are proportional to  $\nu^3$ , while magnetic dipole transition probabilities are proportional to  $\nu$ . The

<sup>17</sup> J. H. Van Vleck, *J. Phys. Chem.* **41**, 67 (1937).

<sup>18</sup> L. J. F. Broer, C. J. Gorter, and J. Hoogschagen, *Physica* **11**, 231 (1945).

<sup>19</sup> B. R. Judd, *Phys. Rev.* **127**, 750 (1962).

<sup>20</sup> G. S. Ofelt, *J. Chem. Phys.* **37**, 511 (1962).

<sup>21</sup> John D. Axe, Jr., *J. Chem. Phys.* **39**, 1154 (1963).

<sup>22</sup> William F. Krupke and John B. Gruber, *Phys. Rev.* **139**, A2008 (1965).

<sup>16</sup> J. L. Prather, *Natl. Bur. Std. (U. S.) Monograph* **19** (1961).

far-infrared frequencies  $\nu$  considered here are two orders of magnitude lower than the optical frequencies associated with intermanifold transitions, so that electric quadrupole transition probabilities will be reduced by a factor of  $10^6$  while the probabilities for magnetic dipole transitions will only be reduced by  $10^2$ . The crystal-field absorption lines are weak, narrow, and immersed in a rich spectrum of phonon lines, hence an accurate measurement of their absorption coefficients is not possible. However, their relative line strengths have been estimated and compared with calculated values of the square of matrix elements of  $J$ , since these are proportional to magnetic dipole transition probabilities.

### ERBIUM ETHYL SULPHATE

The ground configuration of erbium is  $4f^{11}$ , equivalent to three  $4f$  holes, since the closed  $4f$  shell contains 14 electrons. The ground manifold is  $^4I_{15/2}$ , and under the influence of the  $C_{3h}$  crystal field in the ethyl sulphate lattice it splits into eight Kramers' doublets. A brief treatment of the far-infrared results on erbium ethyl sulphate has been given previously,<sup>23</sup> but they will be treated in detail here.

Elliott and Stevens<sup>15</sup> have considered the paramagnetic resonance results for dilute erbium ethyl sulphate, which consist of measurements of  $g_{11}$  and  $g_1$  for the ground doublet. This is not sufficient information to determine four parameters, so they simply choose a set which gives correct  $g$  values.

Although several authors,<sup>24-28</sup> have made spectroscopic measurements, the most complete investigation is the work of Erath,<sup>27</sup> who observed at zero field a total of 46 Stark levels arising from splittings in ten  $J$  manifolds. He then used intermediate coupling operator equivalent factors to make a first order (neglecting  $J$  mixing) calculation of the ground manifold splitting in terms of the four crystal-field parameters. Using his observed splitting for crystals at 77°K, he then evaluated the parameters and obtained  $B_2^0 = 125.8$ ,  $B_4^0 = -81.19$ ,  $B_6^0 = -31.06$ , and  $B_6^6 = 387.19$   $\text{cm}^{-1}$ . These parameters reproduced all the ground manifold levels to a standard deviation of 2.9  $\text{cm}^{-1}$ , and he also calculated the splittings of the excited manifolds and fit all 46 observed Stark levels to a standard deviation of 4.5  $\text{cm}^{-1}$ . While this is fairly satisfactory agreement between theory and experiment, the possibility arose that it could be improved, particularly if a magnetic field were applied and the information obtained on the magnetic character of the states (from the Zeeman splitting) were also used to determine the parameters.

<sup>23</sup> R. G. Wheeler and J. C. Hill, Phys. Letters 20, 496 (1966).

<sup>24</sup> H. Severin, Ann. Physik. 1, 41 (1947).

<sup>25</sup> K. H. Hellwege, S. Hüfner, and H. G. Kahle, Z. Physik 160, 149 (1960).

<sup>26</sup> H. G. Kahle, Z. Physik 161, 486 (1961).

<sup>27</sup> Edward H. Erath, J. Chem. Phys. 34, 1985 (1961).

<sup>28</sup> Eugene Y. Wong, J. Chem. Phys. 39, 2781 (1963).

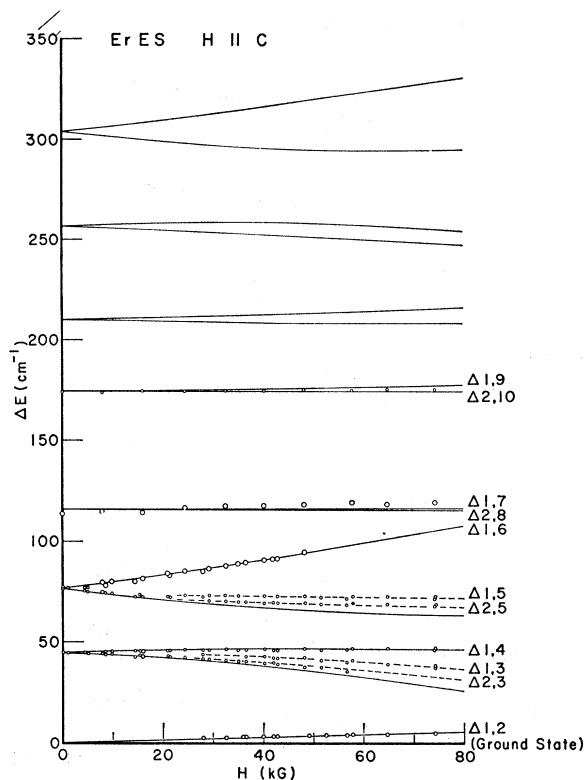


Fig. 4. Calculated and observed transition energies for erbium ethyl sulphate (ErEs) and H||c. The calculated values are represented by solid lines and the measured points by open circles, whose size is indicative of the experimental error.

For a crystal held at a low temperature where only the lowest doublet will have an appreciable population, a maximum of seven transitions within the ground manifold can be observed at zero field. Four of these transitions were actually found. Since for each line the zero-field transition energy and one  $g$  value are both independent data, the information obtained observing the four transitions over a range of applied field is enough to overdetermine the four crystal-field parameters. As a first approximation to the observed splitting a first-order crystal field calculation was made, in which Russell-Saunders operator equivalent factors were used for the reasons discussed above. The least-squares procedure was applied to obtain parameters which gave a good fit between calculated and observed transition energies at 0 and 40 kG. Then the larger, second-order matrix was calculated in which interaction with the first excited  $^4I_{13/2}$  manifold was included. This manifold was taken to lie at 6800  $\text{cm}^{-1}$  as calculated by Erath.<sup>27</sup> The first-order parameters were inserted in the matrix first and the Stark and Zeeman splittings calculated again. As expected from the large separation between the ground and excited manifolds, the changes in the calculated splittings were small, averaging 0.4  $\text{cm}^{-1}$ . However the parameters were again varied by the least-squares method until the best over-all fit was ob-

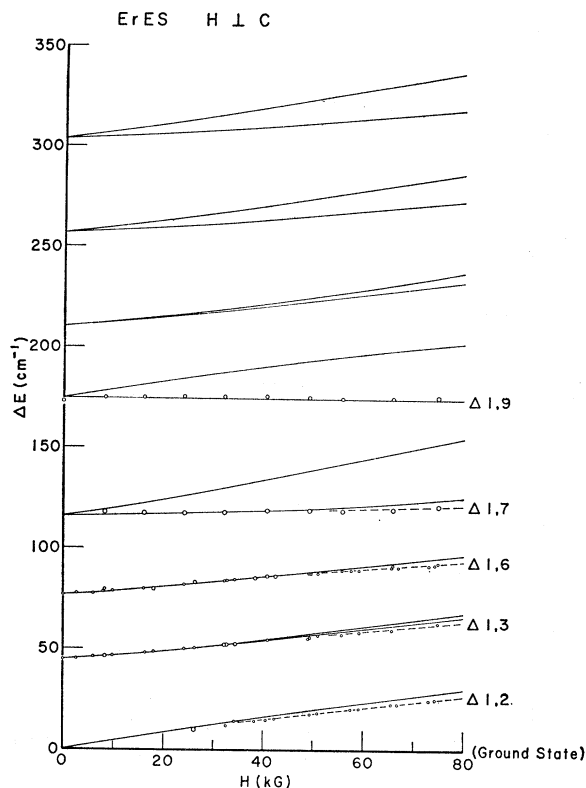


FIG. 5. Calculated and observed transition energies for erbium ethylsulphate (ErES) and  $H \perp c$ .

tained with  $B_2^0 = 118.8$ ,  $B_4^0 = -73.9$ ,  $B_6^0 = -30.4$ , and  $B_6^6 = 375.9 \text{ cm}^{-1}$ .

Graphs were constructed in which the calculated transition energies are plotted as solid lines and the measured transition energies as open circles. The size of the circles is indicative of the experimental uncertainty, which is usually equal to the resolution at which data was obtained. This follows from the fact that the crystal-field linewidths were found to be instrument limited, i.e., they could be reduced when higher resolution data was taken. In cases where a crystal field and phonon line fell at nearly the same frequency, thus reducing the accuracy with which the crystal-field line could be located, the error was correspondingly increased.

The results for erbium are shown in Fig. 4 for  $H \parallel c$  and in Fig. 5 for  $H \perp c$ . It will be seen that in both field orientations no transitions are observed to the three highest doublets. There are some extra lines appearing in the  $H \parallel c$  case. These are  $\Delta 1,3$  and  $\Delta 1,5$  which are attributed to transitions originating on the ground state  $\psi_1$ , rather than on the upper component  $\psi_2$  of the ground doublet. The energy differences between these transitions and the corresponding  $\Delta 2,3$  and  $\Delta 2,5$  are the same at a given field value, and have been used as a measure of the splitting of the ground doublet, since this splitting was below the low-frequency limit of the spec-

trometer. As the field increases and  $\psi_2$  rises in energy it starts to become depopulated and the  $\Delta 2,3$  and  $\Delta 2,5$  transitions become weaker,  $\Delta 2,3$  eventually becoming unobservable.

The agreement between the calculated and observed transition energies is good, the standard deviation  $\delta$  for the levels at zero field and, for both  $H \parallel c$  and  $H \perp c$ , at 40 kG being  $1.2 \text{ cm}^{-1}$ , which is an improvement over Erath's  $\delta$  of  $2.9 \text{ cm}^{-1}$  for his ground manifold calculation. While the standard deviation here is comparable to the experimental uncertainty, there are some deviations which are persistently outside the error. Referring again to Fig. 4 for  $H \parallel c$  this is the case for transitions  $\Delta 2,3$  and  $\Delta 2,5$ . It is interesting to note that the other component in each of these doublets is fit almost perfectly by the crystal-field calculation. Turning to Fig. 5 for  $H \perp c$  one can see that all but one of the transitions deviate appreciably at fields above about 40 kG.

It has proved impossible to eliminate these deviations by varying the field parameters, since the sum of the squares of differences between calculated and observed transition energies was actually minimized by the least-squares procedure. A variation of any one of the four parameters only increased this sum. This also means the possibility of the deviation being due to configuration interaction is eliminated, since Rajnak and Wybourne<sup>29</sup> have shown that within a manifold the effect of configuration interaction is equivalent to a scaling of the parameters. Since the same is true for the effects of intermediate coupling, this too must be eliminated as a cause of the deviations.

The only remaining explanation which seems to make any sense is to attribute the deviations to interaction of either or both of the levels involved in a transition with one or more phonons. This possibility is suggested by the fact that absorption spectra in the visible contain not only electronic transitions, but also these transitions with phonons coupled to them.<sup>4</sup> This implies there is some coupling between the electronic states and the phonons, perhaps of the type described by Satten.<sup>30-32</sup> However, there are several infrared active phonon lines in this spectral region and many of these are crossed by crystal-field lines as the latter shift with the increasing magnetic field. In no case was there evidence of these level crossings involving states which are interacting, i.e., neither the phonon nor the crystal-field line showed any deviations as they approached the crossing point. This implies that any such interaction must be taking place with either an infrared inactive mode or the one active mode allowed by the factor group analysis but not definitely confirmed by observation. Even if the mode were an inactive one, upon being crossed by a Stark level with which it interacts the Stark level

<sup>29</sup> K. Rajnak and B. G. Wybourne, *J. Chem. Phys.* **41**, 565 (1964).

<sup>30</sup> R. A. Satten, *J. Chem. Phys.* **27**, 286 (1957).

<sup>31</sup> R. A. Satten, *J. Chem. Phys.* **29**, 658 (1958).

<sup>32</sup> R. A. Satten, *J. Chem. Phys.* **30**, 590 (1959).

TABLE III. First-order wave functions at  $H=0$  kG for erbium, dysprosium, and samarium ethyl sulphate.

Levels	Erbium	Dysprosium	Samarium
1	$-0.69 +5/2\rangle+0.72 -7/2\rangle$	$-0.05 +15/2\rangle+0.28 +3/2\rangle-0.96 -9/2\rangle$	$- -1/2\rangle$
2	$0.69 -5/2\rangle-0.72 +7/2\rangle$	$0.05 -15/2\rangle-0.28 -3/2\rangle+0.96 +9/2\rangle$	$+ +1/2\rangle$
3	$0.5 -15/2\rangle-0.65 -3/2\rangle+0.57 +9/2\rangle$	$0.51 +5/2\rangle-0.86 -7/2\rangle$	$+ -5/2\rangle$
4	$-0.5 +15/2\rangle+0.65 +3/2\rangle-0.57 -9/2\rangle$	$-0.51 -5/2\rangle+0.86 +7/2\rangle$	$- +5/2\rangle$
5	$-0.86 -15/2\rangle-0.31 -3/2\rangle+0.41 +9/2\rangle$	$-0.08 +13/2\rangle+0.2 +1/2\rangle-0.98 -11/2\rangle$	$- -3/2\rangle$
6	$0.86 +15/2\rangle+0.3 +3/2\rangle-0.41 -9/2\rangle$	$0.08 -13/2\rangle-0.2 -1/2\rangle+0.98 +11/2\rangle$	$+ +3/2\rangle$
7	$0.21 +13/2\rangle-0.87 +1/2\rangle+0.45 -11/2\rangle$	$0.99 -15/2\rangle-0.06 -3/2\rangle-0.07 +9/2\rangle$	
8	$0.21 -13/2\rangle-0.87 -1/2\rangle+0.45 +11/2\rangle$	$0.99 +15/2\rangle-0.06 +3/2\rangle-0.07 -9/2\rangle$	
9	$0.72 +5/2\rangle+0.69 -7/2\rangle$	$0.99 -13/2\rangle-0.13 -1/2\rangle-0.11 +9/2\rangle$	
10	$0.72 -5/2\rangle+0.69 +7/2\rangle$	$0.99 +13/2\rangle-0.13 +1/2\rangle-0.11 -9/2\rangle$	
11	$0.1 +15/2\rangle+0.69 +3/2\rangle+0.71 -9/2\rangle$	$0.86 -5/2\rangle+0.51 +7/2\rangle$	
12	$0.1 -15/2\rangle+0.69 -3/2\rangle+0.71 +9/2\rangle$	$-0.86 +5/2\rangle-0.51 -7/2\rangle$	
13	$0.47 +13/2\rangle-0.32 +1/2\rangle-0.82 -11/2\rangle$	$-0.08 -15/2\rangle-0.96 -3/2\rangle-0.27 +9/2\rangle$	
14	$-0.47 -13/2\rangle+0.32 -1/2\rangle+0.82 +11/2\rangle$	$-0.08 +15/2\rangle-0.96 +3/2\rangle-0.27 -9/2\rangle$	
15	$0.86 -13/2\rangle+0.38 -1/2\rangle+0.34 +11/2\rangle$	$0.14 -13/2\rangle+0.97 -1/2\rangle+0.18 +11/2\rangle$	
16	$0.86 +13/2\rangle+0.38 +1/2\rangle+0.34 -11/2\rangle$	$0.14 +13/2\rangle+0.97 +1/2\rangle+0.18 -11/2\rangle$	

should still show the type of deviation produced in such a crossing. This may be happening with  $\psi_3$  and  $\psi_5$  for  $\mathbf{H}\parallel c$ . As both levels move to lower energies their deviations appear, in the case of  $\psi_5$  the deviation becoming constant as the state levels off.  $\psi_3$ , on the other hand, continues to move toward lower energy and the deviation continues to increase. Since both levels are deviated upward, the interaction would have to be with a phonon lying below  $35\text{ cm}^{-1}$ . However with  $\mathbf{H}\perp c$   $\psi_2$  is observed to move through the  $10\text{--}20\text{ cm}^{-1}$  region without showing any signs of a level crossing in this region. Therefore only the  $5\text{--}10\text{ cm}^{-1}$  and the  $20\text{--}35\text{ cm}^{-1}$  regions can be occupied by such a phonon. When the dysprosium data is considered later, it will be seen that the former region is the most likely.

Turning now to a consideration of the line intensities, calculation of transition probabilities requires knowing the wavefunctions for the states between which transitions occur and these were obtained as part of the process of diagonalizing the crystal-field matrices. Wave functions for all three salts are given in Table III, where for simplicity only first-order wave functions at zero field are listed. Using the wave functions obtained for both field orientations at  $H=40$  kG, the squares of the matrix elements of  $J$ , to which the magnetic dipole transition probabilities are proportional, are easily calculated. For  $\mathbf{H}\parallel c$  the transitions are either pure  $\sigma$  transitions (matrix element of  $J_z$  nonzero) or  $\pi$  transitions (matrix element of  $J_x$ ,  $J_y$  nonzero). For  $\mathbf{H}\perp c$  where the  $J_z$  components of the states can be strongly mixed, a given transition can have both  $\pi$  and  $\sigma$  character, but transitions will be labeled according to which character predominates. The calculated transition probabilities for erbium ethyl sulphate are listed in Table IV, along with the qualitative estimates of the relative line strengths. The agreement is good, for example calculated probabilities for transitions to

states 11 through 16 are either zero or negligibly small, and no transitions were observed to these states. The orientation of the radiation field is such that  $\pi$  transi-

TABLE IV. Comparison of observed and calculated relative magnetic-dipole absorption intensities in erbium ethyl sulphate at  $H=40$  kG.

Transition	Observed intensity	$ \langle\psi_i J \psi_f\rangle ^2$		Polarization
		$H\parallel c$	$H\perp c$	
1,2	... <sup>a</sup>	13.7	0.36	$\pi$
2,3	w	5.9	5.9	$\pi$
1,3	w	0	<0.01	$\pi$
1,4	m	11.8	<0.01	$\pi$
2,5	s	7.5	0	$\pi$
1,5	m	0	0	
1,6	m	1.3	2.9	$\pi$
1,7	w	0	<0.01	$\sigma$
2,8	w	0	<0.01	$\sigma$
1,9	w	9	8.5	$\sigma$
2,10	w	9	0.02	$\sigma$
1,11	...	<0.01	0.03	$\pi$
2,12	...	<0.01	<0.01	$\pi$
1,13	...	0	<0.01	$\pi$
2,14	...	0	<0.01	$\sigma$
2,15	...	0	<0.01	$\sigma$
1,16	...	0	0.02	$\pi$

<sup>a</sup> The transition energy is outside the range of the spectrometer.



tions are always allowed while  $\sigma$  transitions are only very weakly allowed in the  $\mathbf{H}\parallel c$  case. The only transitions which should then show polarization effects are  $\Delta 1,9$  and  $\Delta 2,10$ , and they do so, becoming much weaker for  $\mathbf{H}\parallel c$ .

Since this only represents a check on relative line intensities, an effort was made to measure an absolute line strength and compare it with the line strength calculated for a magnetic dipole transition. The line chosen as presenting a reasonable chance of having a measurable intensity was the  $\Delta 1,6$  transition for  $\mathbf{H}\parallel c$ . At  $H=42.3$  kG this line is fairly well separated from nearby phonons and its absorption coefficient  $\alpha(k)$  was measured as a function of frequency  $k$  (in  $\text{cm}^{-1}$ ). For a magnetic dipole transition the integral of the absorption coefficient over all frequency space is related to the square of the matrix element of  $J$  by<sup>18,22,33</sup>

$$c \int_0^\infty \alpha(k) dk = \rho n \frac{2\pi h k e^2 g_L^2}{3 m^2 c^2} |\langle \psi_i | \mathbf{J} | \psi_j \rangle|^2, \quad (5)$$

where  $\rho$  is the number of rare-earth ions per cubic centimeter,  $n$  is the index of refraction of the medium at the frequency  $k$ ,  $e$ , and  $m$  the electronic charge and mass,  $c$  the speed of light and  $g_L$ , the Lande  $g$  factor for the manifold to which  $\psi_i$  and  $\psi_j$  belong. The right side of Eq. (5) was evaluated using the calculated value of  $|\langle \psi_1 | \mathbf{J} | \psi_6 \rangle|^2$  from Table IV and setting  $n=1.5$  by extrapolation of data given by Krupke and Gruber.<sup>2</sup> The result is

$$\rho n \frac{2\pi h k e^2 g_L^2}{3 m^2 c^2} |\langle \psi_1 | \mathbf{J} | \psi_6 \rangle|^2 \cong 9 \times 10^{12} \text{ cm}^{-1} \text{ sec}^{-1}. \quad (6)$$

The left side was approximated by integrating the measured  $\alpha(k)$  to obtain

$$c \int_0^\infty \alpha(k) dk \approx 25 \times 10^{12} \text{ cm}^{-1} \text{ sec}^{-1}. \quad (7)$$

Consider the error arising from the measurement of  $\alpha(k)$ , this agreement is remarkable. It is taken as definitely confirming the conclusion that the observed transitions are primarily magnetic dipole transitions.

Nevertheless there are still discrepancies as can be seen by referring again to Table IV. For  $\mathbf{H}\parallel c$  lines  $\Delta 1,3$  and  $\Delta 1,5$  should not be observed at all, while transitions to  $\psi_7$  and  $\psi_8$  should not be seen for either field orientation. It is unlikely that configuration interaction can explain these deviations, since it would mix odd parity states into all the Stark components and one would then expect the transitions above  $200 \text{ cm}^{-1}$  to also become observable. Again the most likely possibility appears to be coupling with a low frequency phonon. If an odd parity mode is mixed into either the initial or

final state in a transition, the matrix element for an electric dipole transition will then be nonzero. This is consistent with the fact that for  $\mathbf{H}\parallel c$  the two states  $\psi_3$  and  $\psi_5$  are the terminal states for the induced transitions  $\Delta 1,3$  and  $\Delta 1,5$ , and these are the states whose deviations from the crystal-field calculation have also been attributed to phonon interaction. The turning on of the transition  $\Delta 1,7$  can also be attributed to mixing of  $\psi_7$  with a low frequency phonon, whereas the states above  $200 \text{ cm}^{-1}$  are too far away for such an interaction to induce a transition. It thus remains that most of the observed lines are magnetic dipole transitions, with the remainder probably being induced by phonon interaction.

### DYSPROSIUM ETHYL SULPHATE

Dysprosium has a  $4f^9$  ground configuration, equivalent to having five  $4f$  holes. The ground manifold is  ${}^6H_{15/2}$ , which again splits into eight Kramers doublets in the ethyl sulphate crystal field.

Gramberg<sup>34</sup> investigated the visible absorption spectra and measured the position and  $g$  values for the first two excited Stark components of the ground manifold at  $4.2^\circ\text{K}$ . He also measured the positions, but not the  $g$  values, for an additional two components at  $58^\circ\text{K}$ . Powell and Orbach<sup>35</sup> found a set of parameters which very accurately reproduced the positions of the two lowest excited levels at  $4.2^\circ\text{K}$ , but the average error in  $g$  values was over 10% and ranged as high as 50%. Hüfner<sup>36</sup> also obtained a set of parameters for dysprosium, but only fit the  $58^\circ\text{K}$  splittings and did not give the results of calculating either splittings or  $g$  values for the  $4.2^\circ\text{K}$  data. Again it was felt that if low-temperature data on the behavior of the states over a wide range of applied magnetic field were available, it should be possible to find crystal-field parameters which reproduced not only the zero-field splitting, but also the magnetic behavior.

When the Stark splitting of the entire ground manifold is calculated with a reasonable set of parameters, the doublets divide into two groups. The lower group contains five doublets, including the ground doublet, the highest of these lying at about  $70 \text{ cm}^{-1}$  at zero field. The second, higher group contains three doublets, all above  $150 \text{ cm}^{-1}$ . As was the case with erbium, no transitions were observed to the three levels in the higher group, but transitions from the ground state to the remaining four levels in the lower group were observed. Transitions were seen to at least one member of all four of these doublets over the total range of magnetic field, and this provided sufficient data to determine the field parameters.

A first-order calculation was again made, this time using Hüfner's parameters  $B_2^0=124$ ,  $B_4^0=-79$ ,

<sup>33</sup> A. C. G. Mitchell and M. W. Zemansky, *Resonance Radiation and Excited Atoms* (Cambridge University Press, Cambridge, England, 1961).

<sup>34</sup> G. Gramberg, *Z. Physik* **159**, 125 (1960).

<sup>35</sup> M. J. D. Powell and R. Orbach, *Proc. Phys. Soc. (London)* **A78**, 503 (1961).

<sup>36</sup> S. Hüfner, *Z. Physik* **169**, 417 (1962).

$B_6^0 = -31$ , and  $B_6^6 = 492 \text{ cm}^{-1}$ . These were varied to obtain the best fit to the data, then inserted in a second-order calculation. The position of the next higher  ${}^6H_{13/2}$  manifold was taken as being  $3500 \text{ cm}^{-1}$  as calculated by Wybourne.<sup>37</sup> In this case the average change in the calculated levels was  $2.5 \text{ cm}^{-1}$ , in contrast to  $0.4 \text{ cm}^{-1}$  for erbium. This is not unreasonable in light of the fact that the energy difference to the admixed  $J$  manifold is half what it was for erbium. The least squares procedure was applied and after a few iterations it converged to the parameters  $B_2^0 = 143.9$ ,  $B_4^0 = -85.1$ ,  $B_6^0 = -33.2$ , and  $B_6^6 = 535.4 \text{ cm}^{-1}$ . These represent changes over Hufner's parameters ranging from 7 to 16%.

The resulting fit is shown in Fig. 6 for both  $\mathbf{H} \parallel c$  and  $\mathbf{H} \perp c$ , where the levels to which no transitions were seen have been deleted and the graphs plotted with an expanded energy scale. Calculating the standard deviation as for erbium gives  $\sigma = 1.1 \text{ cm}^{-1}$ , which again is comparable to the experimental uncertainty. Nevertheless, as before there are some deviations outside the range of the experimental error. For  $\mathbf{H} \parallel c$  the discrepancy in line  $\Delta 1,9$  is as high as  $3 \text{ cm}^{-1}$ . For  $\mathbf{H} \perp c$  there is a serious deviation in line  $\Delta 1,3$ , especially above  $40 \text{ kG}$ . Once again the ground doublet splitting was measured indirectly from the difference in the pairs  $\Delta 1,3 - \Delta 2,3$  and  $\Delta 1,4 - \Delta 2,4$ . This time there is also a good deal of error between the calculated and measured ground-doublet splitting.

The best explanation again seems to be interaction with a phonon level in the  $5$  to  $10 \text{ cm}^{-1}$  region. This would explain the deviation in the ground doublet splitting for  $\mathbf{H} \perp c$  because, unlike erbium, the calculated position of the upper component enters well into this region. On this view the depression of the upper component would then be the result of this component attempting to cross a phonon with which it is interacting. The apparent deviation of level  $\psi_3$  can also be accounted for in this scheme. Referring again to Fig. 6, it will be seen that as the field increases the slope of  $\Delta 1,3$ , which is equivalent to that of  $\psi_3$ , quickly changes from negative to positive. This results from the fact that  $\psi_3$  and  $\psi_2$  are coupled by the perpendicular magnetic field, and this coupling is fairly strong. This means that it is strongly affected by the position of  $\psi_2$ . Now assuming the crystal-field calculation is essentially correct, the fairly rapid rise of  $\psi_2$  with field above  $20 \text{ kG}$  will also push  $\psi_3$  up rapidly via the coupling term. If, however, the actual position of  $\psi_2$  is a few wave numbers lower as a result of the phonon interaction, this would relax the coupling to  $\psi_3$ . On a second-order perturbation basis the effect would be through an increase in the energy denominator between  $\psi_3$  and  $\psi_2$ . This in turn would allow the actual position of  $\psi_3$  to be lower, i.e., it would not be deviated so much toward higher energy. A semiquantitative test of this hypothesis can be made

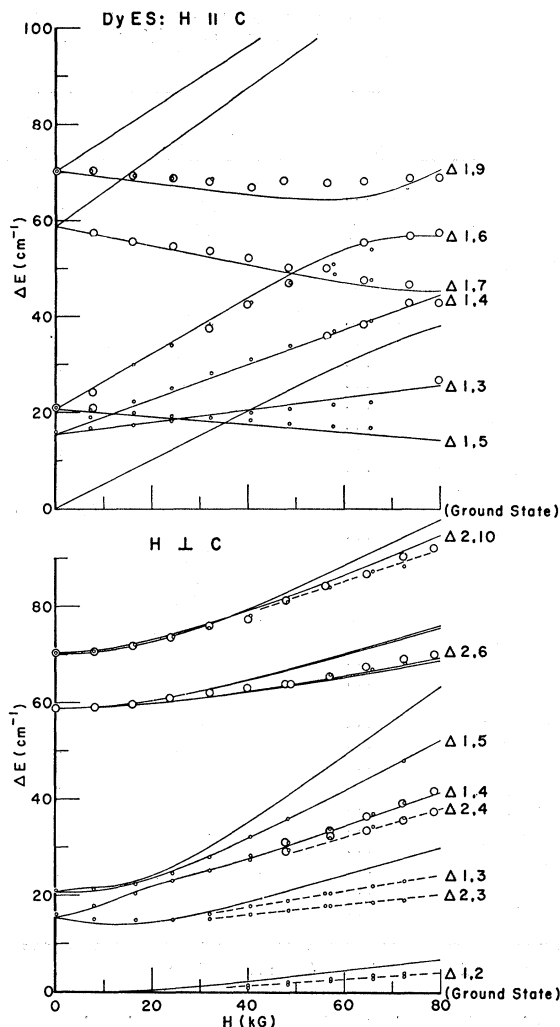


Fig. 6. Calculated and observed transition energies for dysprosium ethylsulphate (DyES).

in the following way. Considering the calculated values at  $80 \text{ kG}$ , the energy denominator or difference  $\psi_3 - \psi_2$  is  $\approx 23 \text{ cm}^{-1}$ . Again by comparison with its calculated position, the depression of  $\psi_2$  by the supposed phonon level is  $\approx 3 \text{ cm}^{-1}$ . Thus the percentage change in the denominator is  $\approx 3 \text{ cm}^{-1} / 23 \text{ cm}^{-1} \approx 13\%$ . Making the very rough assumption that all matrix elements between  $\psi_2$  and  $\psi_3$  are independent of their separation, the change in the second-order perturbation correction to  $\psi_3$  would then be the same as the change in the energy denominator, i.e.,  $\approx 13\%$ . The deviation of  $\psi_3$  from its calculated position is  $\approx 6 \text{ cm}^{-1} / 30 \text{ cm}^{-1} \approx 20\%$ . In light of the assumption on the constancy of the matrix elements between  $\psi_2$  and  $\psi_3$ , this is reasonable agreement.

It would, of course, be desirable to place this entire hypothesis on a much more solid quantitative basis. However this would require knowing the position of the postulated phonon, and unfortunately the spectrometer as it now stands is not capable of supplying

<sup>37</sup> B. G. Wybourne, J. Chem. Phys. 36, 2301 (1962).

TABLE V. Comparison of observed and calculated relative magnetic-dipole absorption intensities in dysprosium ethyl sulphate at  $H=40$  kG.

Transition	Observed intensity	$ \langle\psi_i J \psi_f\rangle ^2$	Polarization
		$H\parallel c$	( $\pi$ only)
1,2	...	0	
1,3	<i>w</i>	11.6	$\pi$
1,4	<i>w</i>	0	
1,5	<i>w</i>	9.7	$\pi$
1,6	<i>w</i>	0	
1,7	<i>w</i>	0	
1,8	...	0.23	$\sigma$
1,9	<i>s</i>	0	
1,10	...	<0.01	$\pi$
1,11	...	0	
1,12	...	0.5	$\pi$
1,13	...	0	
1,14	...	2.3	$\sigma$
1,15	...	0.8	$\pi$
		$H\perp c$	( $\pi$ and $\sigma$ )
1,2	... <sup>a</sup>	13.3	$\sigma$
1,3	<i>w</i>	3.2	$\pi$
2,3	<i>m</i>	2.7	$\sigma$
1,4	<i>s</i>	0.02	$\sigma$
2,4	<i>s</i>	1.8	$\sigma$
1,5	<i>m</i>	4.8	$\pi$
2,5	...	0.06	$\sigma$
1,6	...	0.32	$\sigma$
2,6	<i>s</i>	4.6	$\pi$
2,7	...	0.15	$\sigma$
1,8	...	0.02	$\sigma$
1,9	...	0.26	$\pi$
2,10	<i>s</i>	0.02	$\pi$
1,11	...	1.9	$\sigma$
2,12	...	0.6	$\sigma$
1,13	...	1.2	$\sigma$
2,14	...	1.2	$\sigma$
2,15	...	0.14	$\pi$
1,16	...	<0.01	$\pi$

<sup>a</sup> The transition energy is outside the range of the spectrometer.

meaningful data in the low-frequency region involved. For the moment then, this hypothesis must be considered a qualitative explanation.

In order to consider line intensities second-order wave functions were used to calculate the relative magnetic dipole transition probabilities. These are compared with the estimated relative line strengths in Table V. For  $\mathbf{H}\parallel c$  the observing of transitions  $\Delta 1,3$  and  $\Delta 1,5$  is consistent with their having a fairly large transition probability. With one exception the probabilities for transitions to the three highest doublets, i.e., to states  $\psi_{11}$  through  $\psi_{16}$ , are an order of magnitude lower, thus their not being observed is reasonable. Although  $\Delta 1,14$  has a fairly large probability, it is a  $\sigma$  transition and the orientation of the radiation beam is such that  $\sigma$  transitions are only weakly allowed with  $\mathbf{H}\parallel c$ . However, there are four observed transitions for which the probability is identically zero, and the contrast is especially strong for  $\Delta 1,9$ . On the basis of the same analysis given for erbium, the turning on of these transitions is attributed to phonon interaction. Again this is consistent with the fact that only the levels arising from the lower group of five doublets are affected, the

levels in the upper group not being appreciably influenced. It is also interesting to note that the biggest discrepancy is with the state  $\psi_9$ , and referring again to Fig. 6 this is the state which deviates most from the crystal-field calculation. Furthermore it deviates toward higher energy, consistent with its interacting with a low-energy phonon.

For  $\mathbf{H}\perp c$  the situation is similar, there being several states in the lower group to which transitions can be expected, but also some which appear to be induced, for example  $\Delta 1,4$ . Transition  $\Delta 2,10$  is strongly induced, and this may be a result of interaction of the lower state  $\psi_2$  with the phonon level. Again this is consistent with the discussion above on the deviations between the calculated and observed transition energies for  $\psi_2$  and  $\psi_3$ , in which the deviations are ascribed to coupling between  $\psi_2$  and the phonon level, then to coupling between  $\psi_3$  and  $\psi_2$ .

### SAMARIUM ETHYL SULPHATE

Samarium is the only ion of the three studied to lie in the first half of the rare-earth series. Its ground configuration is  $4f^5$ , which gives rise to a  ${}^6H_{5/2}$  ground manifold. There will then be only three Kramers' doublets in the  $C_{3h}$  field, and therefore a much simpler spectrum.

Hellwege and co-workers<sup>38-40</sup> have studied the optical spectra extensively, making detailed investigations of the Zeeman splitting in several of the excited manifolds. In the ground manifold Lämmermann<sup>38</sup> measured the ground-doublet  $g$  values at 4.2°K, and at liquid-air temperatures found the upper two doublets at 53.8 and 63.6  $\text{cm}^{-1}$ . From polarization and Zeeman-effect studies of transitions to the excited manifolds, she identified the  $J_z$  composition of the ground doublets to be  $\pm\frac{1}{2}$ ,  $\pm\frac{3}{2}$ , and  $\pm\frac{5}{2}$  in order of increasing energy. Hüfner<sup>36</sup> made a crystal-field calculation, but since for the ground manifold the operator equivalent factor for the  $B_6^0$  and  $B_6^6$  terms is zero, his first-order calculation evaluated only  $B_2^0$  and  $B_4^0$ . He fit Lämmermann's splittings perfectly with  $B_2^0=78$  and  $B_4^0=-53$   $\text{cm}^{-1}$ , and also obtained her  $J_z$  composition for the states. However, it will be seen that the  $J_z$  assignment for the upper two doublets was in error.

With  $\mathbf{H}\parallel c$  and to first order, the ratio of the Zeeman splittings of the three states with  $J_z=\pm\frac{1}{2}$ ,  $\pm\frac{3}{2}$ , and  $\pm\frac{5}{2}$  will be 1:3:5. Figure 7 shows the measured splitting for  $\mathbf{H}\parallel c$ , and it is clear that the first excited doublet has the highest  $g$  value, thus it must be the  $\pm\frac{5}{2}$  state, in contraction to Lämmermann's assignment of  $\pm\frac{3}{2}$ . This was further confirmed by the fit obtained with the crystal-field calculation.

For the first-order calculation which involves only  $B_2^0$  and  $B_4^0$ , they could be obtained uniquely by solving

<sup>38</sup> H. Lämmermann, Z. Physik 150, 551 (1958).

<sup>39</sup> A. Friederich, K. H. Hellwege, and H. Lämmermann. Z. Physik 158, 251 (1960).

<sup>40</sup> H. Lämmermann, Z. Physik 160, 355 (1960).

the secular determinant using the measured separation at zero field of  $\psi_3$ ,  $\psi_4$  and  $\psi_5$ ,  $\psi_6$  from the ground state. On the basis of the fact that the separation between the ground and first excited manifolds is only  $1080\text{ cm}^{-1}$ , as calculated by Wybourne,<sup>37</sup> the effect of interaction with this manifold should be appreciable. In order to calculate the second-order matrix, it was necessary to choose reasonable values for  $B_6^0$  and  $B_6^6$ . This was done by interpolating between the best available values in the literature obtained in crystal-field calculations on several other rare-earth ethyl sulphates. By this means  $B_6^0 = -40$  and  $B_6^6 = 575\text{ cm}^{-1}$  were chosen. When the second-order calculation was made, the zero-field positions of the upper doublets changed by 0.9 and  $3.6\text{ cm}^{-1}$ , which is the appreciable change expected. These changes were then subtracted from the first-order calculation of positions, and the corrected positions then used to obtain a new  $B_2^0$  and  $B_4^0$ . After a few iterations this converged to  $B_2^0 = 60.1$  and  $B_4^0 = -63.6\text{ cm}^{-1}$  with  $B_6^0$  and  $B_6^6$  remaining at  $-40$  and  $575\text{ cm}^{-1}$ , respectively. The fit obtained is shown in Fig. 7 and can be seen to be excellent, the standard deviation at 0 and 40 kG being  $0.3\text{ cm}^{-1}$ . On the other hand, it should be pointed out that the values for  $B_2^0$  and  $B_4^0$  are de-

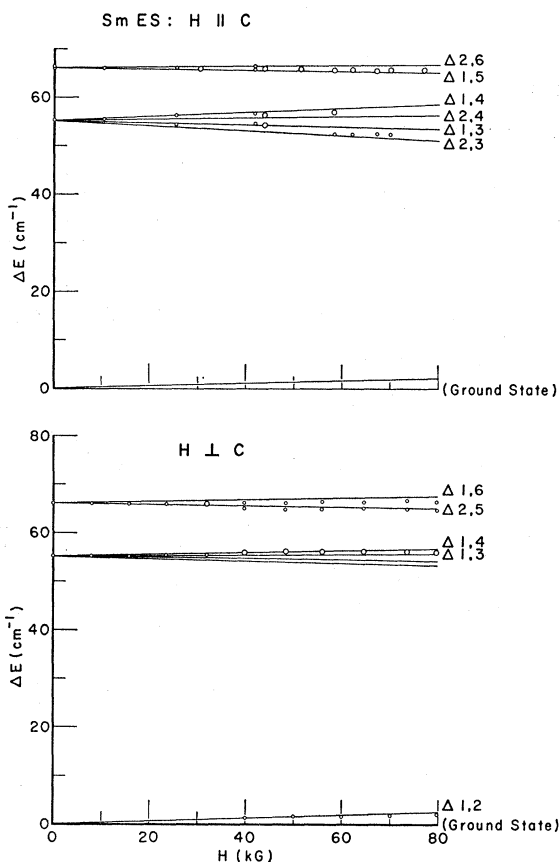


FIG. 7. Calculated and observed transition energies for samarium ethyl sulphate (SmES).

TABLE VI. Comparison of observed and calculated relative magnetic-dipole absorption intensities in samarium ethyl sulphate at  $H = 40\text{ kG}$ .

Transition	Observed intensity	$ \langle \psi_1   J   \psi_f \rangle ^2$	Polarization
$H \parallel c$			
1,3	<i>w</i>	0	( $\pi$ only)
2,3	<i>w</i>	0	
1,4	<i>w</i>	0	
2,4	<i>w</i>	0	
2,5	...	0	
1,5	<i>m</i>	2	$\pi$
2,6	<i>w</i>	2	$\sigma$
1,6	...	0	
$H \perp c$			
1,3	<i>w</i>	<0.01	$\sigma$
1,4	<i>w</i>	<0.01	$\pi$
2,3	...	<0.01	$\pi$
2,4	...	<0.01	$\sigma$
1,5	...	<0.01	$\sigma$
2,5	<i>s</i>	2	$\pi$
1,6	<i>s</i>	1.6	$\pi$
2,6	...	<0.01	$\sigma$

pendent on those chosen for  $B_6^0$  and  $B_6^6$ . The dependence is not a strong one, however, for the change in  $B_2^0$  and  $B_4^0$  over the first-order values is only 1% and 7%.

The question arises as to why agreement between observation and calculation is so much better for samarium than for erbium and dysprosium. The best explanation again lies in phonon interaction, or rather, the lack of it. For both field orientations the ground doublet splitting is very small, being less than  $3\text{ cm}^{-1}$  at 80 kG. Hence there are no states very close to the 5–10- $\text{cm}^{-1}$  region in which an interacting phonon is supposed to be. By the hypothesis developed here, one would then expect the interaction to be appreciably reduced.

Transition probabilities at 40 kG were calculated to produce the results shown in Table VI. For  $H \parallel c$  the presence of  $\Delta 1,5$  and  $\Delta 2,6$  is expected, with  $\Delta 2,6$  being weaker since it is a  $\sigma$  transition. The transitions to  $\psi_3$  and  $\psi_4$  are presumably induced by phonon interaction, possibly with only the lower component  $\psi_1$  of the ground doublet. This agrees with the  $H \perp c$  case where it appears that only transitions originating on  $\psi_1$  are induced.

## CONCLUSION

Using a system built around an interferometric spectrometer far-infrared transitions have been observed between the levels of Stark split ground  $J$  manifolds in three rare-earth ethyl sulphates. Magnetic fields up to 80 kG were applied to the crystals and the Zeeman splitting of the Stark components measured. Sufficient data was obtained for all three salts to allow making an accurate evaluation of the four parameters contained in the crystal-field theory applicable to these compounds. The parameters obtained are collected in Table VII.

TABLE VII. Crystal-field parameters (in  $\text{cm}^{-1}$ ) for erbium, dysprosium, and samarium ethyl sulphate.

Ion	$B_2^0$	$B_4^0$	$B_6^0$	$B_6^6$
Er	118.8	-73.9	-30.4	375.9
Dy	143.9	-85.1	-33.2	535.4
Sm	60.1	-63.6	-40	575

With these parameters the crystal-field theory proved to be very successful in describing both the Stark and Zeeman splitting of the ground manifolds studied, the standard deviation between calculation and measurement being within experimental error. A few significant deviations have been found, most of them occurring for levels with energies below  $80 \text{ cm}^{-1}$ . A hypothesis based on interaction between electronic states and phonons has been developed, and it is capable of qualitatively explaining the deviations.

The intensities of the observed transitions have been studied and have been shown to correlate best with the

assumption that they are primarily magnetic dipole in character. Several observed transitions which cannot be explained this way are considered to be induced by coupling with an odd-parity phonon. It has been found that most of the states to which or from which transitions are induced are also the states whose deviations from the crystal-field calculation have been explained by phonon interaction. If the electron-phonon-coupling hypothesis is sound, it sets a limit on the accuracy which can be obtained by the crystal-field theory. This accuracy has been attained here. However, it would be highly desirable to make a further test of this hypothesis. Since the hypothetical phonon level is believed to lie between 5 and  $10 \text{ cm}^{-1}$ , it would be of interest to obtain meaningful data in this energy range. This would allow searching for absorption produced by an interacting phonon level. If the phonon level is observed in the proper ethyl sulphate, notably that of erbium or dysprosium, its energy should vary as an applied magnetic field is varied. This would then be convincing proof of the postulated electron-phonon interaction.

## Errata

**Theory of Liquid Helium II in a Rotating Annulus: Ginzburg-Pitaevskii Approach**, ALAN J. BENNETT AND L. M. FALICOV [Phys. Rev. **144**, 162 (1966)]. We are grateful to Dr. Klaus Kehr for pointing out a significant error in this work. The treatment of the case of constant angular momentum (Sec. 4) is correct as it stands. For constant rotational frequency (Sec. 3), however, thermodynamic arguments show that the proper quantity to be minimized  $\tilde{F}$  is

$$\tilde{F} = F - \omega \cdot \mathbf{L},$$

where  $F$  is defined in Eq. (2.19). The results of Sec. 3 are then changed to

$$\rho_{sl} = \beta^{-1} \left[ \alpha + \hbar l \omega - \frac{1}{2} m R^2 \omega^2 - \frac{\hbar^2 l^2}{2mR^2} \right] \quad (3.1E)$$

and

$$\tilde{F}(l) = F_{N0} - \frac{1}{2} \beta \rho_{sl}^2 - \frac{1}{2} m \rho R^2 \omega^2. \quad (3.2E)$$

The system behaves in a way similar to that of

Sec. 4, i.e., as the angular velocity is increased states of progressively higher  $l$  are realized. The new thermodynamic function  $\tilde{F}$  attains its minimum value if  $l$  satisfies

$$((mR^2\omega/\hbar) - \frac{1}{2}) \leq l \leq ((mR^2\omega/\hbar) + \frac{1}{2}), \quad (3.3E)$$

and for that regime

$$\rho_{sl}(\omega) = \beta^{-1} [\alpha - \frac{1}{2} m R^2 (\omega - (\hbar l / m R^2))^2]. \quad (3.4E)$$

**Heat Capacity and Other Properties of Hexagonal Close-Packed Helium-4**, D. O. EDWARDS AND R. C. PANDORF [Phys. Rev. **140**, A816 (1965)]. The difference in compressibility between melting and  $0^\circ\text{K}$ , given correctly in Eq. (7) and Table II, should have opposite sign in Table III and Fig. 8. The  $K_0 \times 10^2$  column in Table III should read "0.108, 0.121, 0.140, 0.168, 0.199, 0.236, 0.280, 0.326." With this correction the compressibility at  $0^\circ\text{K}$  is in good agreement with the assumption that the solid is isotropic.